Dynamical control of Mn spin-system cooling by photogenerated carriers in a (Zn,Mn)Se/BeTe heterostructure

J. Debus,[1] A. A. Maksimov,[2] D. Dunker,[1] D. R. Yakovlev,[1,3] I. I. Tartakovskii,[2] A. Waag,[4] and M. Bayer[1]
[1]*Experimentelle Physik 2, Technische Universität Dortmund, 44227 Dortmund, Germany*
[2]*Institute of Solid State Physics, Russian Academy of Sciences, 142432 Chernogolovka, Russia*
[3]*A. F. Ioffe Physical-Technical Institute, Russian Academy of Sciences, 194021 St. Petersburg, Russia*
[4]*Institute of Semiconductor Technology, Braunschweig Technical University, 38106 Braunschweig, Germany*
(Received 27 May 2010; published 31 August 2010)

The magnetization dynamics of the Mn spin system in an undoped (Zn,Mn)Se/BeTe type-II quantum well was studied by a time-resolved pump-probe photoluminescence technique. The Mn spin temperature was evaluated from the giant Zeeman shift of the exciton line in an external magnetic field of 3 T. The relaxation dynamics of the Mn spin temperature to the equilibrium temperature of the phonon bath after the pump-laser-pulse heating can be accelerated by the presence of free electrons. These electrons, generated by a control laser pulse, mediate the spin and energy transfer from the Mn spin system to the lattice and bypass the relatively slow direct spin-lattice relaxation of the Mn ions.

DOI: 10.1103/PhysRevB.82.085448 PACS number(s): 75.50.Pp, 78.55.Et, 78.67.De, 78.20.Ls

I. INTRODUCTION

Diluted magnetic semiconductors (DMSs) based on II-VI compounds with Mn^{2+} ions are regarded as model materials for future spintronics applications.[1,2] The strong *sp-d* exchange interaction between the spins of free carriers and the localized magnetic moments of Mn^{2+} ions provides a variety of magnetic, magneto-optical, and magnetotransport phenomena.[3–5] The spin dynamics of the carriers and the Mn spin system in DMS is controlled by their interaction with each other and with the phonon bath of the crystal lattice. Due to the bright band-edge photoluminescence (PL) in wide band-gap II-VI DMS the dynamics of the carrier-Mn exchange interaction can be suitably studied by optical spectroscopy.

In the past years the dynamical magnetic properties of DMS resulting from spin-spin and spin-lattice relaxation (SLR) mechanisms have been intensively investigated. The strong dependence of magnetization dynamics on the Mn concentration,[6] spin diffusion in heteromagnetic semiconductor structures,[7,8] and acceleration of SLR of Mn ions in the presence of free electrons[9,10] have been reported. The free electrons provide an additional channel for spin and energy transfer from the Mn spin system into the phonon bath (lattice), which can be considerably more efficient than the direct spin-lattice relaxation channel.

In the previous studies stationary methods have been used to change the electron concentration in DMS heterostructures: modulation doping of the barriers with donors[10] and/or application of a gate voltage for fine tuning of the electron density in the quantum well.[9] The electron concentration, however, can be varied in time domain by, e.g., short and intense laser pulses, as it has been realized in (Cd,Mn)Te/(Cd,Mg)Te and (Zn,Mn)Se/(Zn,Be)Se quantum wells with a type-I band alignment.[11,12] Nevertheless, due to the short recombination time of the photogenerated carriers in these structures it was not possible to reach the condition of the cold carrier system and to clearly detect the effect of the carrier-assisted cooling of the Mn spin system by photogenerated carriers.

In this paper we report on the dynamically controllable acceleration of SLR, leading to a cooling of the Mn spin system, by the generation of photocarriers in a $Zn_{0.99}Mn_{0.01}Se/BeTe$ heterostructure with a type-II band alignment. The distinctive feature of the studied structure is the spatial separation of the thermalized electrons and holes in the $Zn_{0.99}Mn_{0.01}Se$ and BeTe layers, respectively. This results in very long radiative recombination times of $\gtrsim 100$ ns for photocreated electrons.[13,14] A $Zn_{0.99}Mn_{0.01}Se/BeTe$ multiple quantum well (MQW) structure was examined under pulsed photoexcitation by means of time-resolved photoluminescence. It has been ascertained that the relaxation process of the Mn spin system can be accelerated on the nanosecond time scale by optical tuning of the electron concentration in the $Zn_{0.99}Mn_{0.01}Se$ layers.

II. EXPERIMENTAL DETAILS

We have studied a nominally undoped $Zn_{0.99}Mn_{0.01}Se/BeTe$ MQW structure, denoted by the label CB1963. The sample was grown by molecular-beam epitaxy on a (100)-oriented GaAs substrate. It contains ten periods of alternating 20-nm-thick $Zn_{0.99}Mn_{0.01}Se$ and 10-nm-thick BeTe layers.

To study the dynamical response of the Mn ion magnetization on a laser impact, a finite equilibrium magnetization is induced by an external magnetic field. The excess kinetic energy of the photoexcited carriers, being transferred into the Mn spin system, causes an increase in the Mn spin temperature T_{Mn}. The relaxation of T_{Mn} back to its equilibrium with the lattice temperature is detected by time-resolved PL.[6] As the Mn spin temperature controls the giant Zeeman shift of the heavy-hole exciton state, the exciton energy in magnetic field is used for the evaluation of T_{Mn}. The heavy-hole exciton energy is measured from the spectral position of its right-handed (σ^+) circularly polarized PL line.

In our optical measurements the sample was immersed in pumped liquid helium at a temperature of $T=1.8$ K and was exposed to magnetic fields up to 8 T. The magnetic field **B**

was applied in the Faraday geometry parallel to the sample growth axis (**z** axis): **B**∥**z**. The spin dynamics of the Mn spin system was studied by a pump-probe technique implementing three pulsed lasers with pump, control, and probe functions, respectively. Initially, the sample was excited by a 5 ns pulse of the third harmonic of a Q-switched $Nd:YVO_4$ laser (3.49 eV), denoted by pump pulse in the following. The typical pump power density amounted to 200 kW/cm^2. The pump generated hot photocarriers which in the course of their energy and spin relaxation heated the Mn spin system. After a time delay of 150 μs the sample was excited by a control pulse of 8 ns duration. It was provided by the third harmonic of a Nd:YAG laser with a photon energy of 3.49 eV and an excitation density ranging from 0.1 to 150 kW/cm^2. The control pulse created photocarriers which assisted in the cooling of the Mn spin system. The dynamics of the Mn spin temperature was measured by the energy shift of the exciton PL line. For that purpose, weak probe-laser pulses with a photon energy of 3.06 eV, generated by a semiconductor laser, were used. The pulse duration was adjusted to a few tens of microseconds, whereby the excitation density was kept below 100 mW/cm^2 in order to avoid an additional heating of the Mn spins. For the time-resolved detection of the PL signals a gated charge-coupled device camera with a time resolution of 2 ns was used. The camera was connected to a 0.5 m spectrometer and synchronized with the laser pulses by means of a digital pulse delay generator.

III. RESULTS

Figure 1(a) shows the band alignment of the type-II (Zn,Mn)Se/BeTe heterostructure.[15] Due to the large direct band gap of BeTe ($E_{\mathrm{BeTe}} \approx 4.5$ eV) the laser excitation in the ultraviolet spectral range (3.06 or 3.49 eV) generates photocarriers in the (Zn,Mn)Se layers ($E_{\mathrm{ZnMnSe}} \approx 2.8$ eV) only. After the photogeneration electrons become localized in the (Zn,Mn)Se layers and holes scatter within $\tau_{\mathrm{rel}} \approx 10$ ps into the BeTe layers[16] where they have minimal potential energy.

The spatial carrier separation is demonstrated in PL spectra by the emission lines of the direct and indirect optical transitions. A direct emission at about 2.8 eV, which is attributed to the recombination of electron-hole pairs in the (Zn,Mn)Se layers, is denoted by D in Fig. 1(a). Its temporal decay is controlled by the radiative recombination of excitons and the hole scattering out of the (Zn,Mn)Se layers. An indirect (ID) emission at about 1.8 eV is contributed by electrons from (Zn,Mn)Se and holes from BeTe. The large conduction-band and valence-band offsets of about 2 eV and 1 eV, respectively, result in a very small penetration of the carrier wave functions into the neighboring layers. This drastically reduces the overlap of the electron and hole wave functions leading to a very long radiative recombination time for the indirect transition expanding up to few hundreds of nanoseconds.[13,16] Since the giant Zeeman shift of the direct emission line provides information about the magnetization relaxation and Mn spin temperature due to the *sp-d* exchange interaction in (Zn,Mn)Se, in this paper we focus on the study of the dynamics of the direct emission line.

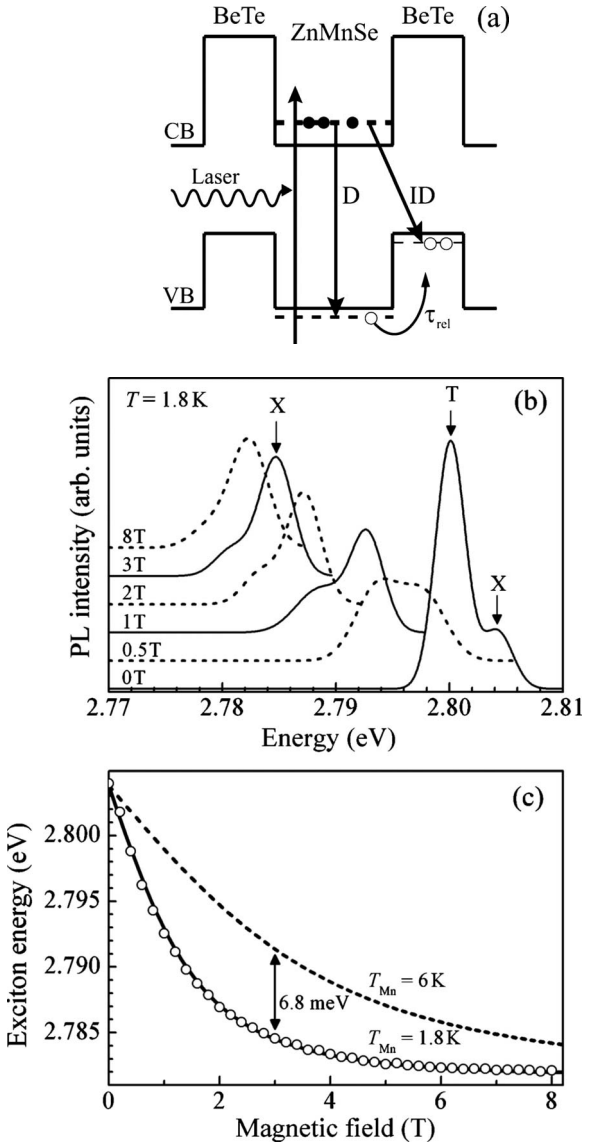

FIG. 1. (a) Schematic band alignment of (Zn,Mn)Se/BeTe type-II heterostructure. Arrows represent direct (D) and indirect (ID) in space PL transitions. Photogenerated holes are scattered into BeTe layers lowering their potential and kinetic energy. (b) PL spectra of direct transition in $Zn_{0.99}Mn_{0.01}Se$/BeTe sample for different magnetic fields. Exciton (X) and trion (T) lines are marked by arrows. (c) Giant Zeeman shift of heavy-hole exciton state for two different spin temperatures T_{Mn} of Mn system. The experimental data (open circles) are attributed to PL spectra, which are shown in panel (b). T_{Mn} was derived from a fitting of the Zeeman shift using Eqs. (1) and (2) with $S_{\mathrm{eff}}=2.43$ and $T_0=0.9$ K.

In Fig. 1(b) σ^+ polarized PL spectra of the direct transition are depicted for different magnetic fields under low continuous-wave photoexcitation with a density of 15 mW/cm^2. The emission line at 2.804 eV (at $B=0$ T) is related to the recombination of heavy-hole excitons (X), the second line, which is shifted by 4.9 meV to lower energy from the exciton, can be attributed to trion (T) recombination. Here, the trion is a negatively charged exciton complex consisting of two electrons and one hole. The energy shift between the lines is consistent with the trion binding energy

in ZnSe-based QWs.[17] For magnetic fields $B<2$ T the small exciton and trion linewidth of $\lesssim 3$ meV allows a clear distinction between the both PL lines. With increasing magnetic field the trion PL intensity is redistributed in favor of the exciton one. This is a result of the trion ionization, which takes place when the giant Zeeman splitting of the conduction-band electrons exceeds the trion binding energy.[18]

Note, the formation of the negatively charged excitons requires the presence of excess (resident) electrons in the (Zn,Mn)Se layers. Since the studied structure is nominally undoped the resident electron concentration is very small in the dark conditions. It is confirmed by the very weak trion oscillator strength measured in the reflectivity spectrum (not shown here). In PL experiments under continuous-wave excitation a finite concentration of the excess electrons in the (Zn,Mn)Se layers is formed due to the spatial carrier separation. From the relative intensities of the exciton and trion PL lines we estimate that the concentration of the excess electrons is about 10^9 cm^{-2}.

The giant Zeeman shift of the heavy-hole exciton with increasing magnetic field up to 8 T is shown by symbols in Fig. 1(c). It is commonly described by the following equation:[6]

$$E_X(B) = E_X(B=0) + \frac{1}{2}(\delta_e\alpha - \delta_h\beta)N_0 x\langle S_z\rangle, \qquad (1)$$

where $E_X(B=0)$ is the exciton energy in the absence of an external magnetic field, $N_0\alpha=0.26$ eV and $N_0\beta=-1.31$ eV are the exchange constants for the conduction and valence bands,[19] respectively, and x is the Mn content. The parameters δ_e and δ_h account for the overlap of the carrier wave functions with the DMS layer and in our case they were taken as $\delta_e=\delta_h=1$. $\langle S_z\rangle$ represents the thermal average value of the Mn spin along the magnetic field direction for a Mn spin temperature T_{Mn}. It is generally expressed by the modified Brillouin function $B_{5/2}$,

$$\langle S_z\rangle = -S_{eff}B_{5/2}\left[\frac{5}{2}\frac{g_{Mn}\mu_B B}{k_B(T_0+T_{Mn})}\right]. \qquad (2)$$

Here $g_{Mn}=2.01$ is the g factor of the Mn^{2+} ions, μ_B is the Bohr magneton, and k_B is the Boltzmann constant. S_{eff} and T_0 are the parameters for the effective Mn spin and effective Mn temperature which allow to phenomenologically describe the effect of the antiferromagnetic interactions between neighboring Mn ions.

The experimental data in Fig. 1(c) can be well fitted by Eq. (1), as it is shown by the solid line, with a fit parameter of $T_{Mn}=1.8$ K, which corresponds to the bath temperature of the lattice. Therefore, we conclude that under this excitation condition the Mn spin system is in equilibrium with the lattice. In order to illustrate the Mn heating effect on the giant Zeeman shift we plot the calculated shift for $T_{Mn}=6$ K by the dashed line. One can see that the shift is considerably reduced in comparison to the case of $T_{Mn}=1.8$ K, e.g., at a magnetic field of 3 T it is smaller by about 7 meV. This demonstrates that the giant Zeeman shift of the exciton emission in DMS structures can serve as a very sensitive tool to evaluate the Mn spin temperature. We will use this tool here to study the magnetization dynamics.

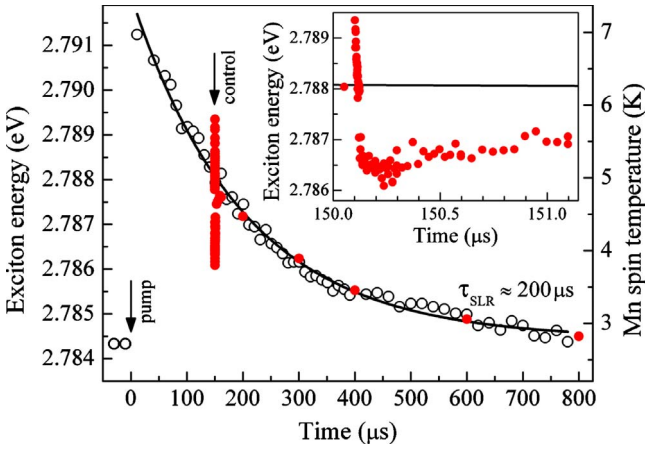

FIG. 2. (Color online) Temporal evolution of the exciton energy with (closed circles) and without (open circles) the control pulse impact with a power of 5 kW/cm^2, $B=3$ T and $T=1.8$ K. A monoexponential fit (solid line) yields the spin-lattice relaxation time $\tau_{SLR}\approx 200$ μs. The pump pulse impact is set at zero delay and the control pulse excites the sample at $t_c=150$ μs, both are marked by arrows. The probe pulse with a duration of 25 μs is shifted sequentially to cover the whole time range. The inset provides an enlarged view on the Zeeman shift shortly after t_c, indicating an acceleration of the spin-system cooling by means of the control pulse. The solid line in the inset is the same as in the main panel.

In Fig. 2 the temporal evolution of the exciton energy and the Mn spin temperature at $B=3$ T and $T=1.8$ K is shown for two optical excitation schemes: the excitation of the sample with a pump pulse, illustrating the SLR process (open circles) for one initial heating impact, and the additional excitation with a control pulse delayed in time from the pump pulse (closed circles). Due to the low Mn concentration ($x=0.01$) the SLR process exceeds the characteristic lifetime of nonequilibrium phonons of a few microseconds.[6] Hence, the SLR time τ_{SLR} can be extracted from the temporal shift of the exciton energy. An exponential fit of the experimental data, shown by the solid line in Fig. 2, gives us $\tau_{SLR}\approx 200$ μs. This value is in close agreement with the published data for undoped type-I (Zn,Mn)Se-based heterostructures.[6] It also shows that in the studied structure the effect of the resident electrons on the acceleration of the SLR is very small and can be neglected.

The Mn spin system is initially driven out of its equilibrium state corresponding to $T_{Mn}=1.8$ K by the pump pulse which arrives at zero time delay. The control pulse excites the sample at $t_c=150$ μs after the pump pulse, when the Mn spin system is not yet relaxed to the equilibrium with the lattice, see Fig. 2. The Mn magnetization dynamics is influenced by the control pulse in two ways (see inset of Fig. 2): a strong increase in the exciton energy, which corresponds to the increase in T_{Mn}, is followed by a rapid decrease, where the exciton resonance moves below the solid line level evidencing the Mn cooling in the presence of photogenerated carriers. At these time delays relative to the control pulse holes are already scattered into BeTe and only electrons,

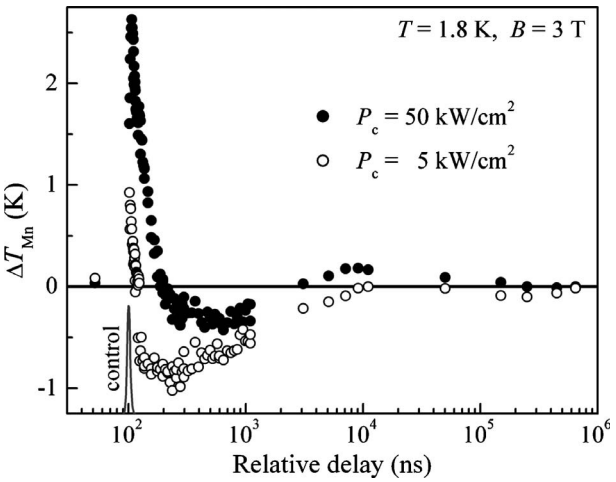

FIG. 3. Deviation of the Mn spin temperature induced by the control pulse of two different powers (symbols) in respect to the evolution of the Mn spin temperature after the pump pulse only (solid line). Temporal dependence of the deviation relative to the control pulse incidence is shown. According to the logarithmic time scale we have chosen the control pulse position at 100 ns. The decrease in T_{Mn} ranges from the relative delay of 5 to 300 ns dependent on the power density P_c of the control pulse. The overall change in ΔT_{Mn} can be separated into characteristic relaxation regimes related to heating and cooling effects in the Mn spin system.

staying in $Zn_{0.99}Mn_{0.01}Se$, can induce the Mn cooling.

One should note here that in experiments with pulsed laser excitation the energy shifts of the emission lines can be caused by many-body effects, like phase-space filling and band-gap renormalization.[20] These effects should weakly depend on the magnetic field. In our experimental conditions at zero magnetic field we have checked that we did not reach the regimes, where these effects should be taken into account. At zero magnetic field neither a broadening of the neutral exciton PL line nor an attenuation of its intensity compared to the trion PL line has been observed up to maximal powers of the control pulse. Moreover, for the typically used control power of 5 kW/cm^2 a spectral shift of the exciton PL line was not visible during the control pulse action at $B=0$ T. Even for the high control pulse power of 100 kW/cm^2 the exciton line shows energy shifts up to 1.5 meV only during the pulse impact. At time delays after the control pulse, where the Mn spin temperature has been evaluated, these energy shifts do not exceed 0.3 meV, which is by one order of magnitude less than the typical spectral shifts due to heating and cooling of the Mn spin system at an applied magnetic field of about 3 T.

In more detail the effect of the control pulse is presented in Fig. 3, where the energy shift of the exciton line, taken as the difference between the spectral positions at zero magnetic field and at $B=3$ T, is already converted to the Mn spin temperature. The temporally evolved difference ΔT_{Mn} of the Mn spin temperatures measured with and without the control pulse impact is given for two excitation densities. For the presentation a logarithmic time scale has been chosen and the incidence of the control pulse has been shifted from $t_c=150$ μs to 100 ns. The temporal evolution of the Mn spin temperature shows different relaxation regimes after the control pulse impact:

(i) It is increased during the control pulse action, which is demonstrated by positive values of ΔT_{Mn} exceeding 2 K. The Mn spin system is heated by carriers photogenerated by the control pulse.

(ii) 0 ns$<t<$300 ns. The Mn spin temperature decreases from positive to negative values of ΔT_{Mn} indicating the cooling of the Mn spins induced by the control pulse. The long-living thermalized photoelectrons in the $Zn_{0.99}Mn_{0.01}Se$ layers, which are spatially separated from the holes, provide a bypass relaxation channel for the Mn spin system to the lattice. We estimated that for $P_c=5$ kW/cm^2 the electron concentration in the $Zn_{0.99}Mn_{0.01}Se$ layers is about 10^{10} cm^{-2}.

(iii) $t>300$ ns. After approximately 300 ns the ΔT_{Mn} values start to increasingly approach the zero level. At these time delays most of the photogenerated electrons have been already recombined with the holes and the relaxation processes are solely controlled by the spin dynamics of the Mn spin system. The zero level, shown by the solid line in Fig. 3, corresponds to the nonequilibrium T_{Mn} induced by the pump pulse. The recovery of the Mn spin temperature to this level after the control pulse action evidences that the carrier-induced cooling is spatially inhomogeneous and addresses local regions of the Mn spin system.[11,21–23] The spin diffusion in the Mn spin system leads to a restoration of the homogeneous Mn spin temperature in the $Zn_{0.99}Mn_{0.01}Se$ layer.[8] The effect of the control pulse is vanished for $t>10$ μs. At these delays the Mn spin system follows the regular cooling process via spin-lattice relaxation.

Let us discuss the laser-induced cooling effect of the Mn spin system corresponding to the regime (ii). In external magnetic fields the spin-lattice relaxation of the Mn ions requires a coupled transfer of spin and energy from the Mn ions to the phonon system. However, in II-VI DMS with low Mn concentrations the relaxation process is quite slow due to the very weak interaction of the isolated Mn^{2+} ions with the phonons.[6,24] In the studied structure with $Zn_{0.99}Mn_{0.01}Se$ layers the SLR time is approximately 200 μs, as one can see in Fig. 2. The presence of free electrons in DMS layers offers an additional channel for transferring spin and energy from the Mn ions into the lattice. This channel is very efficient as, on the one hand, the electrons are strongly coupled with the Mn ions via exchange interaction and, on the other hand, efficient electron-phonon interaction provides a fast dissipation of the excess electron energy into the phonon bath with typical times not exceeding 100 ps. The bypassing relaxation channel involving the energy and spin reservoirs of the thermalized electrons is active within the electron lifetime, which in our case of the heterostructure with a type-II band alignment covers few hundreds of nanoseconds. Obviously, the efficiency of this channel is controlled by the density of photocreated electrons.

The electron density and, respectively, the cooling efficiency of the Mn spin system can be tuned by the intensity of the control pulse. In Fig. 4 the Mn spin temperature is shown as a function of the control pulse power P_c. The right scale of this figure provides the corresponding exciton energies from which T_{Mn} was evaluated. For low excitation densities ($\leq$0.5 kW/cm^2) the Mn spin system is only slightly influ-

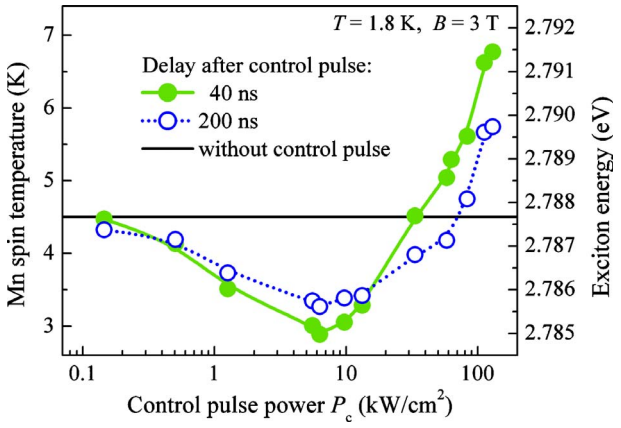

FIG. 4. (Color online) Mn spin temperature at two different times after the control pulse impact in dependence on the control laser power. At 6 kW/cm^2 and for a delay of 40 ns the spin temperature is reduced from 4.5 to 2.9 K. For very high excitation densities the Mn spins are overheated. At the delay of 200 ns the heating is less efficient.

enced by the control pulse due to a small concentration of photogenerated carriers of about 10^9 cm^{-2}. Laser pulses with power densities 1 kW/cm^2 $< P_c <$ 20 kW/cm^2, creating more than 10^{10} cm^{-2} photoelectrons, induce a pronounced cooling effect. It is well detected at both 40 and 200 ns delays after the control pulse impact. It confirms that the efficient transfer of spin and energy from the Mn ions to the lattice mediated by the thermalized electrons lasts for the electron lifetime. In comparison to the unaffected spin temperature level of 4.5 K the magnitude of the spin cooling amounts to approximately 1.5 K.

For excitation densities exceeding 30–70 kW/cm^2 only an increased Mn spin temperature has been observed. At these high excitation powers at least two mechanisms screen the cooling effect. On the one hand, the cooling effect is saturated with increasing electron concentration, when the regime of a degenerate electron gas with $E_F > k_B T$ is reached. In this case only the part of the electrons, whose energy falls into the $k_B T$ range in the vicinity of the Fermi level E_F, can mediate the spin and energy transfer between Mn ions and phonon system.[6,10] On the other hand, the heating impact by the photogenerated carriers is so strong that the cooling effect, induced by the thermalized electrons, is not sufficient to reduce the Mn spin temperature below the unaffected level of 4.5 K.

IV. DISCUSSION

We first address the rather unexpected behavior of ΔT_{Mn} in the regime (iii). As it is illustrated in Fig. 3, for $t > 300$ ns the Mn spin system is heated up and returns to the same spin temperature as it would have without control pulse impact, see level shown by the solid line. This behavior is observed for the both control pulse power densities. It cannot be explained by a possible contribution of nonequilibrium acoustic phonons generated by photocarriers since the maximum of the phonon population is already reached at 100 ps after the control pulse action and, subsequently, the population only decays. Also, the electrons cannot provide the cooling of the Mn spin system below the level controlled by the nonequilibrium phonons. The nonmonotonic behavior, presented in Fig. 3, can be only related to a spatial inhomogeneity of T_{Mn}, which is induced by the carrier cooling of the Mn spin system and then is washed out by the spin diffusion in the Mn spin system from warmer to colder regions.[11,21–23] The efficiency of the spin diffusion has been very recently analyzed experimentally and theoretically for different types of DMS heterostructures.[8]

We suggest the following explanation for the nonmonotonic behavior of $\Delta T_{Mn}(t)$, presented in Fig. 3. In principle, both hot electrons and hot holes can contribute to the Mn heating. The hole-Mn energy transfer is more efficient due to the larger exchange constant compared to the electron-Mn one. As a result, the hole contribution dominates for the type-I quantum well structures. However, in the type-II structure studied here the holes escape from the $Zn_{0.99}Mn_{0.01}Se$ layers during few picoseconds after photogeneration and, therefore, we suggest that the Mn heating is dominantly provided by the photoelectrons.

The electrons being excited by the control pulse thermalize to the bottom of the conduction band in the $Zn_{0.99}Mn_{0.01}Se$ layer and are localized there by a potential formed by alloy and layer width fluctuations. By further thermalization to the lattice temperature the electrons heat the Mn spin system locally. Since typical relaxation times of the electrons with the emission of acoustic phonons do not exceed 100 ps, the Mn heating by the hot electrons takes place only during the action of the control pulse with 8 ns duration.

When the electron temperature decreases below T_{Mn} the very same electrons reverse their functionality and start to cool the Mn spin system, thus serving as the efficient bypassing channel for the energy and spin transfer from the Mn spins to the lattice. In the local regions the electrons cool the Mn spin system during their lifetime of about 300 ns. The local T_{Mn} is controlled by a balance between the electron-mediated relaxation (cooling) and by the spin diffusion from surrounding regions which do not contain electrons (heating). After the recombination of the electrons, the spin diffusion restores the homogeneous Mn spin temperature in the whole $Zn_{0.99}Mn_{0.01}Se$ layer, which takes about 10 μs. It is worthwhile to note here that for time delays longer than 300 ns the electrons, which contribute to the photoluminescence signal, are photogenerated by the probe pulse. At shorter delays their concentration is relatively small compared to the electrons generated by the control pulse. Nevertheless, the electrons, generated by the control and probe pulse, are localized in the very same places and we are following the spin dynamics of the Mn system in the same local regions. From the heating time of a few microseconds and the characteristic spin-diffusion coefficients, reported in Ref. 8, one can estimate that the size of the localization regions does not considerably exceed 10–20 nm.

In summary, the magnetization relaxation of an initially excited (Zn,Mn)Se/BeTe heterostructure has been accelerated by optical injection of free electrons. The type-II band alignment of the studied structure was essential for providing thermalized electrons with sufficiently long lifetimes in DMS

layers. Within their lifetime of a few hundreds of nanoseconds they open an efficient bypassing relaxation channel for transferring the spin and energy from the Mn spin system to the phonon bath. The laser-induced cooling of the Mn spin temperature can be controlled by the optical excitation density and by the temporal application of the impact pulse.

ACKNOWLEDGMENTS

This work was supported by the Deutsche Forschungsgemeinschaft via Schwerpunktprogramm SPP 1285, the EU Seventh Framework Programme (Grant No. 237252, Spin-optronics), and by the Russian Foundation of Basic Research (Grants No. 08-02-01302 and No. 10-02-00549). The research stay of A.A.M. in Dortmund has been supported by the Deutsche Forschungsgemeinschaft via Grant No. YA65/10-1.

[1] *Semiconductor Spintronics and Quantum Computation*, edited by D. D. Awschalom, D. Loss, and N. Samarth (Springer, Berlin, 2002).
[2] *Spin Physics in Semiconductors*, edited by M. I. Dyakonov (Springer, Berlin, 2008).
[3] J. K. Furdyna, J. Appl. Phys. **64**, R29 (1988).
[4] *Diluted Magnetic Semiconductors*, Semiconductors and Semimetals Vol. 25, edited by J. K. Furdyna and J. Kossut (Academic, London, 1988).
[5] T. Dietl, *Diluted Magnetic Semiconductors*, Handbook on Semiconductors Vol. 3b, edited by S. Mahajan (North-Holland, Amsterdam, 1994), p. 1252.
[6] M. K. Kneip, D. R. Yakovlev, M. Bayer, A. A. Maksimov, I. I. Tartakovskii, D. Keller, W. Ossau, L. W. Molenkamp, and A. Waag, Phys. Rev. B **73**, 045305 (2006).
[7] A. V. Scherbakov, A. V. Akimov, D. R. Yakovlev, W. Ossau, L. Hansen, A. Waag, and L. W. Molenkamp, Appl. Phys. Lett. **86**, 162104 (2005).
[8] A. A. Maksimov, D. R. Yakovlev, J. Debus, I. I. Tartakovskii, A. Waag, G. Karczewski, T. Wojtowicz, J. Kossut, and M. Bayer, Phys. Rev. B **82**, 035211 (2010).
[9] M. K. Kneip, D. R. Yakovlev, M. Bayer, T. Slobodskyy, G. Schmidt, and L. W. Molenkamp, Appl. Phys. Lett. **88**, 212105 (2006).
[10] A. V. Scherbakov, D. R. Yakovlev, A. V. Akimov, I. A. Merkulov, B. König, W. Ossau, L. W. Molenkamp, T. Wojtowicz, G. Karczewski, G. Cywinski, and J. Kossut, Phys. Rev. B **64**, 155205 (2001).
[11] M. G. Tyazhlov, V. D. Kulakovskii, A. I. Filin, D. R. Yakovlev, A. Waag, and G. Landwehr, Phys. Rev. B **59**, 2050 (1999).
[12] M. K. Kneip, D. R. Yakovlev, M. Bayer, A. A. Maksimov, I. I. Tartakovskii, D. Keller, W. Ossau, L. W. Molenkamp, and A. Waag, Phys. Rev. B **73**, 035306 (2006).
[13] S. V. Zaitsev, V. D. Kulakovskii, A. A. Maksimov, D. A. Pronin, I. I. Tartakovskii, N. A. Gippius, M. Th. Litz, F. Fisher, A. Waag, D. R. Yakovlev, W. Ossau, and G. Landwehr, JETP Lett. **66**, 376 (1997).
[14] S. V. Zaitsev, A. A. Maksimov, I. I. Tartakovskii, D. R. Yakovlev, M. Bayer, and A. Waag, Phys. Rev. B **76**, 035312 (2007).
[15] D. R. Yakovlev, C. Sas, B. König, L. Hansen, W. Ossau, G. Landwehr, L. W. Molenkamp, and A. Waag, Appl. Phys. Lett. **78**, 1870 (2001).
[16] A. A. Maksimov, I. I. Tartakovskii, D. R. Yakovlev, M. Bayer, and A. Waag, JETP Lett. **83**, 141 (2006).
[17] G. V. Astakhov, D. R. Yakovlev, V. P. Kochereshko, W. Ossau, W. Faschinger, J. Puls, F. Henneberger, S. A. Crooker, Q. McCulloch, D. Wolverson, N. A. Gippius, and A. Waag, Phys. Rev. B **65**, 165335 (2002).
[18] V. D. Kulakovskii, M. G. Tyazhlov, S. I. Gubarev, D. R. Yakovlev, A. Waag, and G. Landwehr, Il Nuovo Cimento D **17**, 1549 (1995).
[19] A. Twardowski, M. von Ortenberg, M. Demianiuk, and R. Pauthenet, Solid State Commun. **51**, 849 (1984).
[20] J. Shah, *Ultrafast Spectroscopy of Semiconductors and Semiconductor Nanostructures* (Springer, Berlin, 1999).
[21] D. Keller, D. R. Yakovlev, Th. Gruber, A. Waag, W. Ossau, L. W. Molenkamp, F. Pulizzi, P. C. M. Christianen, and J. C. Maan, Phys. Status Solidi B **229**, 797 (2002).
[22] F. Teppe, M. Vladimirova, D. Scalbert, T. Wojtowicz, and J. Kossut, Phys. Rev. B **67**, 033304 (2003).
[23] M. Vladimirova, D. Scalbert, and C. Misbah, Phys. Rev. B **71**, 233203 (2005).
[24] A. V. Akimov, A. V. Scherbakov, and D. R. Yakovlev, in *Handbook of Semiconductor Nanostructures and Nanodevices*, edited by A. A. Balandin and K. L. Wang (American Scientific, Los Angeles, 2006), Vol. 3, Chap. 2, p. 45.